

NASA TECHNICAL NOTE



NASA TN D-6169

C.1

NASA TN D-6169

LOAN COPY: RETI  
AFWL (DOG)  
KIRTLAND AFB,

0132996



TECH LIBRARY KAFB, NM

# NEUTRONIC DESIGN FOR A LITHIUM-COOLED REACTOR FOR SPACE APPLICATIONS

*by Charles L. Whitmarsh, Jr.*

*Lewis Research Center*

*Cleveland, Ohio 44135*



0132996

1. Report No. NASA TN D-6169	2. Government Accession No.	3. Recipient's Catalog No.	
4. Title and Subtitle NEUTRONIC DESIGN FOR A LITHIUM-COOLED REACTOR FOR SPACE APPLICATIONS		5. Report Date February 1971	
		6. Performing Organization Code	
7. Author(s) Charles L. Whitmarsh, Jr.		8. Performing Organization Report No. E-5775	
9. Performing Organization Name and Address  Lewis Research Center National Aeronautics and Space Administration Cleveland, Ohio 44135		10. Work Unit No. 120-27	
		11. Contract or Grant No.	
12. Sponsoring Agency Name and Address  National Aeronautics and Space Administration Washington, D. C. 20546		13. Type of Report and Period Covered Technical Note	
		14. Sponsoring Agency Code	
15. Supplementary Notes			
16. Abstract  <p>Neutronic design calculations were performed for a lithium-7 cooled nuclear reactor concept for space application. Performance goals were 2.17 megawatts thermal for 50 000 hours with a coolant outlet temperature of 1222 K. The reactor was fueled with enriched uranium nitride and controlled by rotation of six fueled drums. The fuel was zoned radially to reduce local power peaking and to enhance reactivity worth of the control system. Local power in the core was limited by a 1-percent-creep criterion established for the fuel cladding. Total control swing was 8.51-percent <math>\Delta k/k</math>. Power distributions, core characteristics, and accident effects were calculated.</p>			
17. Key Words (Suggested by Author(s)) Nuclear reactors Fast nuclear reactors Liquid-cooled reactors Liquid-metal-cooled reactors		18. Distribution Statement Unclassified - unlimited	
19. Security Classif. (of this report) Unclassified	20. Security Classif. (of this page) Unclassified	21. No. of Pages 40	22. Price* \$3.00

# NEUTRONIC DESIGN FOR A LITHIUM-COOLED REACTOR FOR SPACE APPLICATIONS

by Charles L. Whitmarsh, Jr.

Lewis Research Center

## SUMMARY

The neutronic design is presented for a lithium-7 ( $\text{Li}^7$ )-cooled reactor concept for space application. Performance goals are a power output of 2.17 megawatts thermal for 50 000 hours with a coolant outlet temperature of 1222 K (2200 R).

The reactor core consists of a cylindrical arrangement of 247 fuel pins (93.2 per-cent enriched uranium nitride (UN) clad with the tantalum alloy T-111) of which 66 are in six control drums located symmetrically around the core. Control is achieved by rotation of fuel into and out of the stationary core. In the space between the drums is a stationary reflector made from the molybdenum alloy TZM. The core, drums, and reflector are contained in a T-111 pressure vessel. End reflectors of TZM are provided. Nominal dimensions of the core are 19 centimeters (48.3 in.) radius and 38 centimeters (96.5 in.) length with 9-centimeter- (22.9-in. -) thick radial reflectors and 5-centimeter- (12.7-in. -) thick axial reflectors.

A fuel-loading arrangement of 0.355, 0.377, and 0.42 core volume fraction of UN, respectively, in radial zones from the center out to the drums provided sufficient excess multiplication and a control swing of 8.51-percent  $\Delta k/k$ . Control swing requirements in percent  $\Delta k/k$  were 1.47 for fuel loss, 1.09 for temperature defect, 0.95 for axial fuel growth, and 4.39 for shutdown margin. A control curve (reactivity against drum rotational position) was calculated, from which the beginning-of-life drum position of  $118^\circ$  from shutdown was obtained.

Radial power distributions were calculated for drum positions between beginning and end of life. These distributions indicated that fuel loading in the drum pins was limited by a design criterion of  $\leq 1$ -percent creep in the fuel cladding. Core characteristics such as neutron lifetime, effective delayed neutron fraction, and core spectra were calculated. In addition, reactivity effects of loss of coolant, water immersion, fuel melting, and fuel bowing accidents were considered.

## INTRODUCTION

The need for substantial amounts of electric power for space missions has been widely recognized. At Lewis Research Center, programs are underway to develop the required technology for a space power system using a nuclear reactor as the heat source. Early efforts were devoted to consideration of various types of reactors (refs. 1 to 3), although the fast-spectrum, liquid-metal-cooled reactors were attractive from the start. Low weight and long life requirements favored the fast-spectrum cores because of the inherent small size and high fuel density of this reactor type.

However, the amount of reactivity to be controlled led to studies of various methods of providing this control margin (refs. 3 to 10). Moving fuel, external reflectors and moderators, and internal reflectors and moderators were considered for control systems, in addition to fuel zoning to augment the control range.

In order to coordinate the various nuclear design efforts with the material and thermodynamic design efforts, a reference reactor for further system study was selected. Basic operational requirements for the reactor are that it provide 2.17 megawatts of heat for 50 000 hours with a coolant outlet temperature of 1222 K (2200 R) to a Brayton-cycle power conversion system. After review of the work up to this point and consideration of the operating requirements of the power system, a liquid-metal-cooled, refractory-metal reactor with a rotating fueled-drum control system was adopted as a reference design.

The purpose of this report is to present the results of the neutronic analysis of this reference reactor design. Primary efforts were devoted to fuel zoning, control system analysis, and power distribution calculations. Also included are data on accident analyses, kinetics parameters, and flux spectra. All data are the result of analyses based on multigroup transport theory calculations of static reactor models.

The design philosophy followed herein was to ensure that sufficient reactivity was available to exceed minimum requirements in order to allow for unforeseen reactivity requirements that may occur in later stages of design. For example, engineering fabrication tolerances generally exceed those estimated by reactor analysts.

## DESCRIPTION OF REACTOR

The reactor consists of an array of fuel pins, surrounded by a reflector and a pressure vessel, with single-pass coolant channels (fig. 1). In the reference design, 181 fuel pins are arranged in a six-pointed star shape to represent the stationary part of the core. Sixty-six additional fuel pins are distributed in six movable control drums (fig. 2). The fuel is uranium nitride (UN) with the uranium being enriched to 93.2 atomic

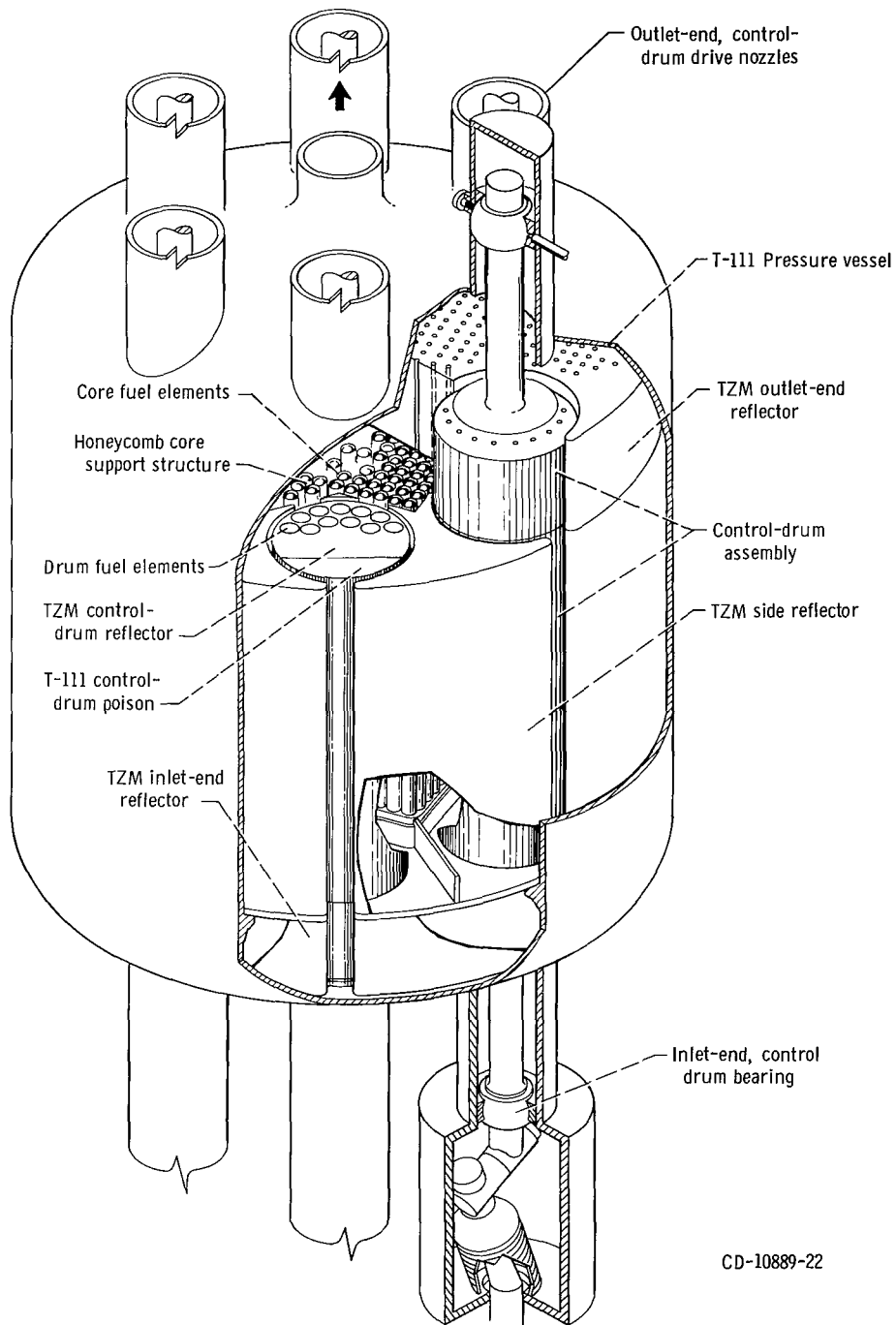


Figure 1. -Reactor schematic.

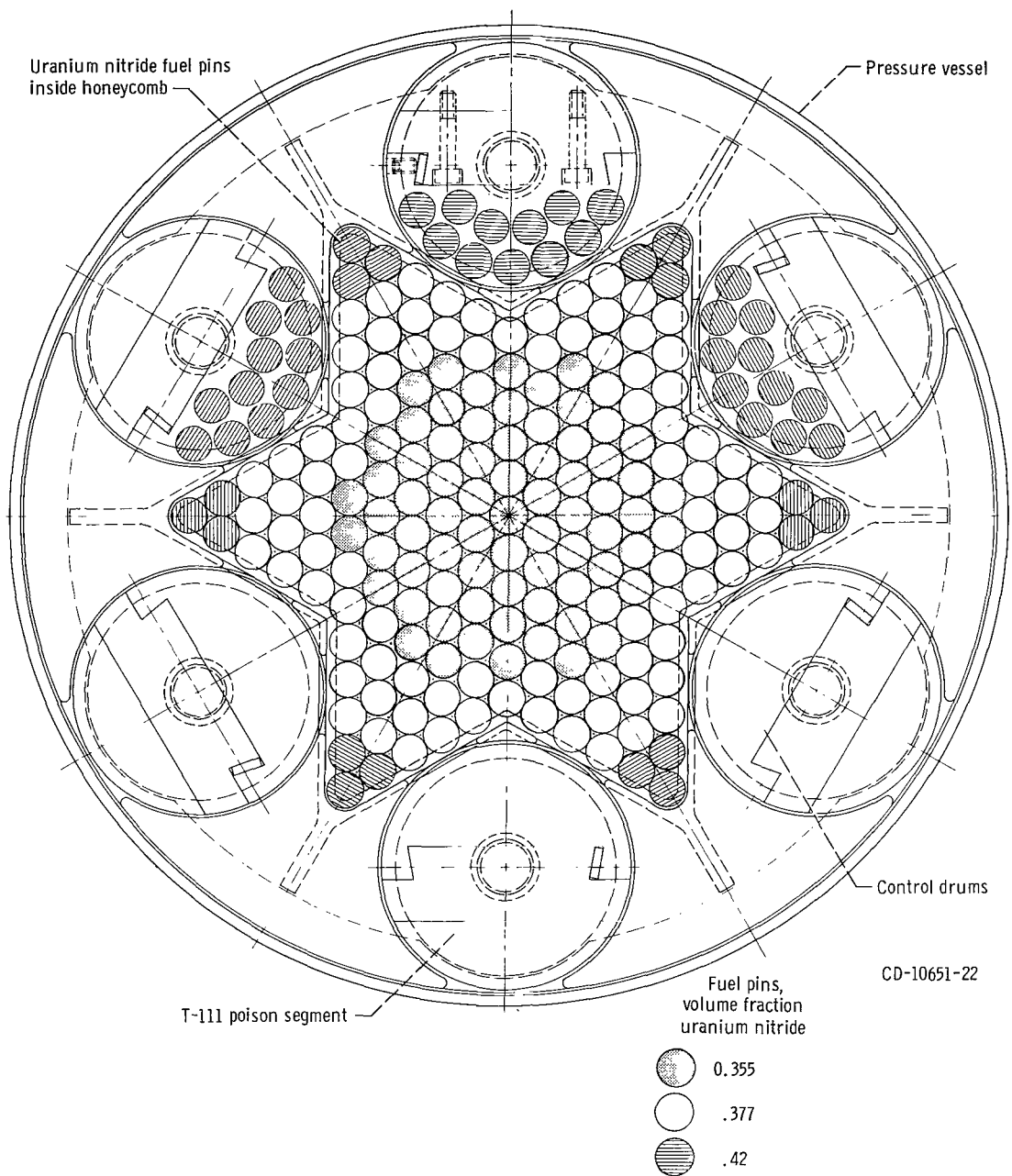
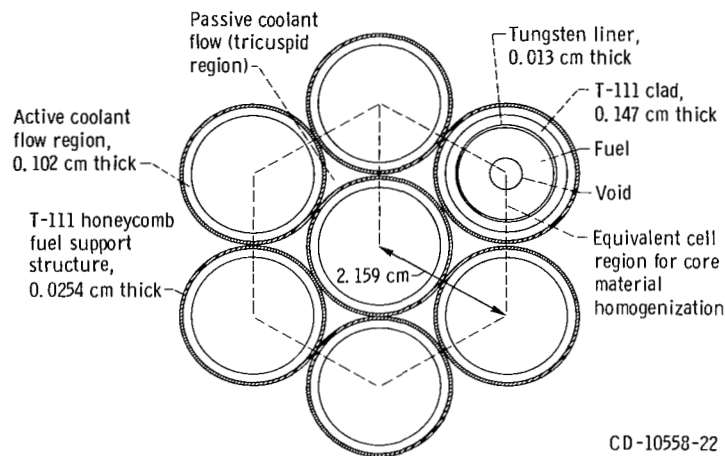


Figure 2. - Cross section of reactor core.

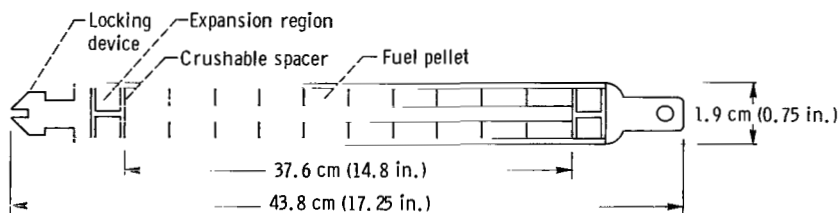
percent of uranium-235 ( $U^{235}$ ) and the fuel cladding is T-111 (a tantalum alloy). The stationary fuel is surrounded by a fixed reflector of TZM (a molybdenum alloy) and six control drums. Each control drum contains a reflector, T-111 as a poison, and fuel. The core is contained in a 0.635-centimeter- (0.25-in. -) thick, T-111 pressure vessel.

Fuel zoning has been shown in a previous study (ref. 7) to be desirable for externally controlled, creep-limited reactors. Therefore, the pins are grouped as follows: zone I includes the central 73 pins, zone II the next 90 pins (in the stationary part nearest the core center), and zone III includes the 18 stationary core pins located on the star points (three pins in each point) and the 66 drum pins. The distribution of fuel between these zones was determined in the design calculations.

The stationary pins are separated into a triangular lattice by a tubular honeycomb structure of T-111 with 0.0254-centimeter- (10-mil-) thick walls (fig. 3(a)). The honeycomb forms 0.102-centimeter- (40-mil-) wide coolant channels around each fuel pin through which 88 percent of the  $Li^7$  coolant flows. The remaining coolant flows at a reduced rate through the tricuspid region between the honeycomb tubes (ref. 10). Total coolant flow rate is 9.4 kilograms per second (20.7 lb/sec).



(a) Lattice and pin cross section.



(b) Fuel pin.

Figure 3. - Fuel-pin design.

Fuel-pin construction includes an active zone of 37.592 centimeters (148 in.) filled with 10 fuel pellets and with expansion regions at each end (fig. 3(b)). Fuel pellets are cylindrical with an axially concentric hole designed to provide space for the fuel to swell. This geometry produces a lower fuel temperature than a solid pellet with comparable swelling space arranged as a peripheral gap. Fuel zoning can be accomplished by varying the hole diameter, which in turn varies the amount of fuel in the pin. The expansion regions and central hole also represent space for fission gas. Locking mechanisms at each end increase overall length to 43.8 centimeters (17.25 in.). The fuel cladding is 0.147-centimeter- (58-mil-) thick T-111 with a 0.013-centimeter- (5-mil-) thick tungsten (W) liner. The pin outside diameter is 1.912 centimeters (0.75 in.). The two locking mechanisms connect to grid plates of T-111. Adjacent to each grid plate is a 5.08-centimeter- (2-in. -) thick TZM axial reflector.

The control system consists of six drums spaced evenly around the core (fig. 2). Each drum contains 11 fuel pins and a segment of T-111 which acts as a neutron poison. Reactivity is controlled by rotating the fuel into and out of the core. The drums are constructed with TZM and are operated by individual drive motors placed external to the pressure vessel. Drum fuel pins are identical to stationary fuel pins except that coolant channels are bored into the drums instead of being formed by a honeycomb structure.

A single-pass coolant flow is used and an attempt has been made to keep the number of different materials to a minimum. For example, T-111 was used for fuel cladding, structure, pressure vessel, and drum poison. Although no shield is shown in the figures, it is anticipated that one will be required. The reactivity effects of a closely coupled shield have been accounted for in the calculations described in the next section by explicitly including a 7.62-centimeter- (3-in. -) thick layer of lithium hydride ( $\text{Li}^6\text{H}$ ) around the radial periphery of the reactor.

## CALCULATIONAL PROCEDURE

All criticality calculations were made with the TDSN (ref. 11) and the DOT (ref. 12) neutron transport programs. The cross sections for these calculations were generated with the GAM program (ref. 13) for energy groups above 0.414 electron volt and with the GATHER program (ref. 14) for energy groups below 0.414 electron volt. All cross sections were flux weighted over the spectrum that would be present in the particular region of their use; for example, core cross sections over a core spectrum, and so forth. For the most part 13- and 4-group energy splits were used, the details and adequacy of which are described in references 4 and 8. Computer running time was reduced by not including a thermal group ( $0 < E < 0.414$  eV) in these sets. The thermal group was considered unnecessary because the lack of moderating materials in most situations cal-



culated herein precluded the existence of a significant number of neutrons in that energy range. Isolated cases requiring a thermal group utilized 14- and 5-group energy splits.

Transport calculations were performed with code options ranging from 1D  $S_4P_0$  13 group to 2D  $S_2P_0$  4 group in order to effect a reasonable tradeoff between accuracy, computer running time, and computer storage limitations. The notation scheme for code options can be described as follows: 1D is a one-dimensional approximation of the real geometry,  $S_4$  represents the angular quadrature of fourth order for solving the  $S_n$  transport equations,  $P_0$  represents cross sections which contain a correction to approximate nonisotropic scattering based on a calculational scheme using only the first term of a Legendre polynomial expansion solution to the transport equation, and 13 group is the number of discrete energy groups for which the multigroup transport equation will be solved. Reactivity corrections between the various levels of calculational sophistication were determined (table I). These data are useful in estimating higher-order (more accurate) results from lower-order calculations. In addition, based on critical experiment analyses (ref. 15), an undefined bias of +2.9-percent  $\Delta k/k$  exists in the criticality calculations reported herein. This bias is believed to be caused by errors in cross sections of molybdenum.

The three calculational geometries used are shown in figure 4. Radial regions can be well represented by either XY or  $R\theta$  models, but neither can adequately represent axial regions. The RZ model can represent axial regions but requires that all radial regions be cylindricized, a considerable distortion from real geometry. One-dimensional calculations used the RZ model for radial zones and an extrapolated height (core height

TABLE I. - COMPARISON OF CODE INPUT OPTIONS  
IN CRITICALITY CALCULATIONS

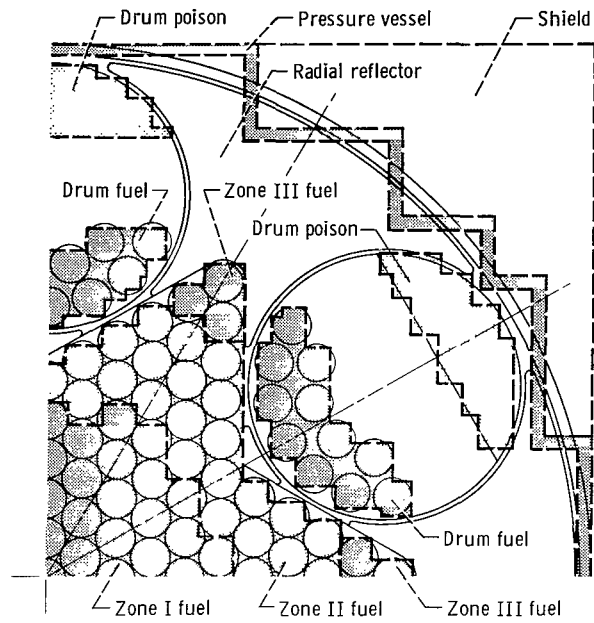
Parameter	Code input <sup>a</sup>	Percent $\Delta k$	Percent $\Delta k/k$
$S_2 - S_4$	1D $S_2$ 4 group - 1D $S_4$ 4 group	-0.60	-0.50
$S_2 - S_4$	RZ $S_2$ 4 group - RZ $S_4$ 4 group	-1.04	-.86
$S_2 - S_4$	$R\theta$ $S_2$ 4 group - $R\theta$ $S_4$ 4 group	-.57	-.47
$S_2 - S_4$	XY $S_2$ 4 group - XY $S_4$ 4 group	.36	.30
4 Group - 13 Group	1D $S_4$ 4 group - 1D $S_4$ 13 group	-.22	-.18
RZ <sup>b</sup> - XY <sup>c</sup>	RZ $S_4$ 4 group - XY $S_4$ 4 group	-.12	-.10
$R\theta$ <sup>d</sup> - XY	$R\theta$ $S_4$ 4 group - XY $S_4$ 4 group	-.78	-.65

<sup>a</sup>All calculations were performed on a drums-rotated-full-in reactor configuration, and all cross sections were  $P_0$  transport corrected.

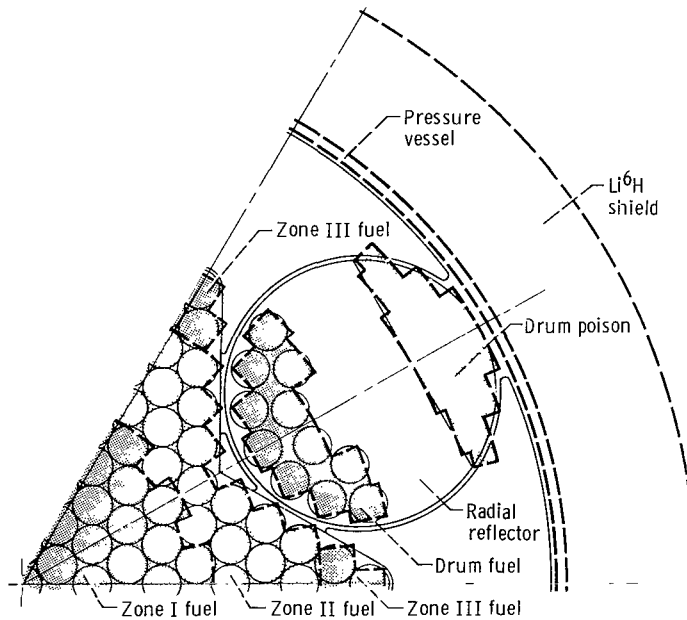
<sup>b</sup>Two-dimensional cylindrical geometry using radial and axial dimensions.

<sup>c</sup>Two-dimensional geometry using Cartesian coordinates in the radial plane.

<sup>d</sup>Two-dimensional cylindrical geometry using radial and azimuthal dimensions.

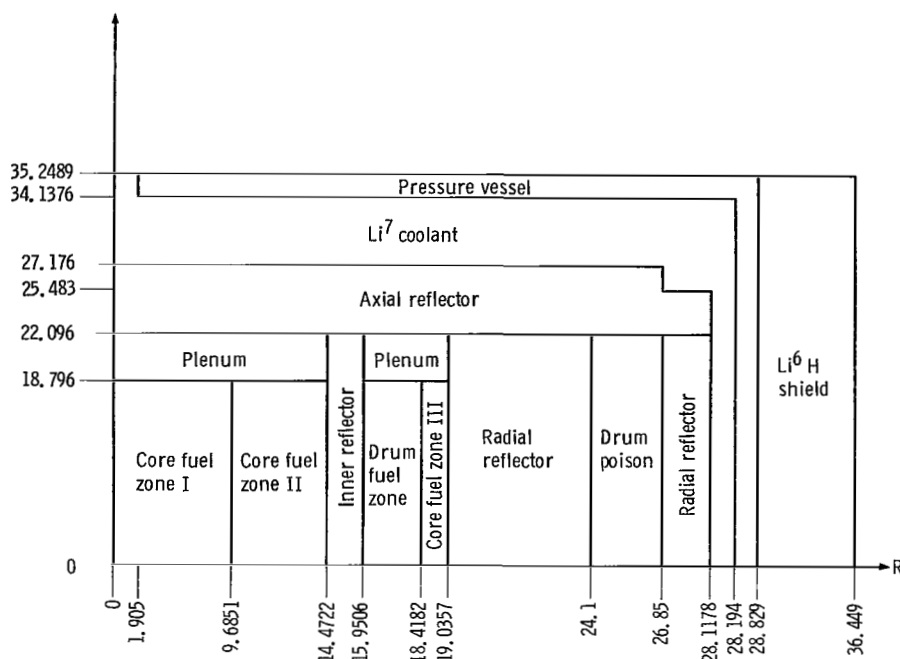


(a) XY model.



(b) Rθ model.

Figure 4. - XY, Rθ, and RZ calculational models of reactor with drums rotated in.



(c) RZ model. (Dimensions are in centimeters.)

Figure 4. - Concluded.

plus reflector savings) to approximate all axial zones. The procedure followed to determine the reflector savings was to do an XY calculation with an assumed reflector savings. Then, with material volumes in each zone preserved, radial dimensions were adjusted to get the same multiplication factor  $k$  from a one-dimensional radial calculation. An RZ calculation with the cylindricized radial geometry and real axial dimensions was performed to obtain the correct reflector savings. Material mixtures for these calculations are itemized in tables II and III.

Reactivity values reported herein were generally based on two noncritical reactor configurations. Thus, the definition for reactivity becomes

$$\text{Percent } \frac{\Delta k}{k} = \frac{k_2 - k_1}{k_1 k_2} \times 100$$

where  $k_1$  is the multiplication constant of the reference configuration and  $k_2$  is the multiplication constant of the perturbed reactor.

Power distributions are reported as  $P/\bar{P}$ , the ratio of local power to the power produced in an average fuel pin. The calculational model used for these calculations was based on room-temperature dimensions and material densities even though the reactor

TABLE II. - MATERIALS FOR XY AND Rθ CALCULATIONAL MODELS

Material	Density, g/cm <sup>3</sup>	Volume percent in-							
		Fueled zone				Radial reflector	Drum poison	Pressure vessel	Shield
		I	II	III	Drum				
U <sup>235</sup> N	14.2	35.5	37.7	42.0	42.0	--	---	---	---
Li <sup>7</sup>	.516	25.2	25.2	25.2	15.9	5	---	---	---
TZM <sup>a</sup>	10.2	----	----	----	13.5	93	---	---	---
T-111 <sup>b</sup>	16.72	24.4	24.4	24.4	20.2	--	100	100	---
W	19.3	1.5	1.5	1.5	1.5	--	---	---	---
Li <sup>6</sup> H	.8	----	----	----	----	--	---	---	100

<sup>a</sup>TZM - 99.42 wt. % Mo, 0.5 wt. % Ti, and 0.08 wt. % Zr; assumed to be pure Mo in all calculations.

<sup>b</sup>T-111 - 89.2 wt. % Ta, 8.5 wt. % W, and 2.3 wt. % Hf.

TABLE III. - MATERIALS FOR ID RADIAL AND 2D RZ MODELS

Material	Density, g/cm <sup>3</sup>	Volume percent in-											
		Fueled zone				Inner reflector	Radial reflector	Drum poison	Cool- ant	Pressure vessel	Plenum	Axial reflector	Shield
		I	II	III	Drum								
U <sup>235</sup> N	14.2	35.5	37.7	42.0	42.0	----	----	----	---	---	--	--	--
Li <sup>7</sup>	<sup>a</sup> .516	25.2	25.2	25.2	15.9	16.4	4.3	----	100	---	47	3	10
TZM	10.2	----	----	----	13.5	83.6	92.9	45.4	---	---	--	97	15
T-111	16.72	24.4	24.4	24.4	20.2	----	----	54.6	---	100	33	--	--
W	19.3	1.5	1.5	1.5	1.5	----	----	----	---	---	--	--	--
Li <sup>6</sup> H	.8	----	----	----	----	----	----	----	---	---	--	--	70

<sup>a</sup>Density at 460 K.

TABLE IV. - EFFECT OF CALCULATIONAL METHOD ON  
RADIAL POWER DISTRIBUTION IN A REACTOR WITH  
CONTROL DRUMS ROTATED FULL IN

Pin location <sup>a</sup>	Reactor at room temperature		Reactor at operating temperature, S <sub>2</sub> P <sub>0</sub> 4 group
	S <sub>4</sub> P <sub>0</sub> 4 group	S <sub>2</sub> P <sub>0</sub> 4 group	
	Ratio of local power to average power		
0-A	1.24	1.25	1.24
1-A	1.23	1.25	1.24
2-B	1.21	1.22	1.22
2-C	1.21	1.22	1.22
3-B	1.16	1.17	1.17
3-C	1.17	1.19	1.18
4-C	1.11	1.11	1.11
4-D	1.13	1.13	1.13
4-E	1.13	1.13	1.13
5-C	1.08	1.08	1.08
5-D	1.15	1.14	1.13
5-E	1.07	1.07	1.07
6-E	1.05	1.05	1.05
6-F	1.07	1.07	1.07
6-G	1.07	1.07	1.07
7-F	.97	.97	.97
7-G	.99	.98	.98
8-H	.88	.88	.88
8-I	.90	.89	.90
9-I	.86	.86	.86
10-K	.74	.73	.73
1-4	1.00	.99	.99
1-5	.97	.97	.97
1-6	.85	.85	.85
1-7	.73	.73	.73
2-3	.86	.85	.85
2-4	.75	.75	.75

<sup>a</sup>See fig. 18.

would be at operating temperature when at power. The use of room-temperature power distributions to represent the reactor at operating temperature ( $\sim 1220$  K) is justified by data presented in table IV. Also shown in table IV is the negligible effect of using higher-order  $S_4$  calculations. Insignificant changes (from  $S_2$  room-temperature results) are noted in either case.

## DESIGN REQUIREMENTS

The principal constraints for the design are that sufficient reactivity be available for  $1.09 \times 10^4$  megawatt hours of operation, that sufficient control be available for safe shutdown at any time, that 1-percent creep not be exceeded in the fuel cladding, and that the reactor be stable under operating and credible accident conditions.

Design procedure generally represents an iterative effort between requirements and performance. Although the data in this section in many cases are based on the final core loading, this does not indicate a fortuitous choice but merely represents the last iteration in the study.

### Reactivity

The reactivity required for operation is categorized as follows: fuel burnup, temperature defect, fuel swelling, and shutdown margin. Summation of these items provides the minimum reactivity capability requirement of the control system.

Fuel loss. - Total fuel consumption by fission to produce 2.17 megawatts for 50 000 hours is 4.77 kilograms of  $U^{235}$ . This assumes that each fission yields 200 million electron volts and that no fissions occur in  $U^{238}$ . (Calculation of the reference design indicated that  $>99.5$  percent of the fissions were in  $U^{235}$ .) Based on the reference-design fuel loading of 181.9 kilograms  $U^{235}$  (206.7 kg UN), average fuel burnup by fission is 2.62 percent of the  $U^{235}$ . In addition to fission, fuel atoms are destroyed by parasitic absorption of neutrons. For the reference design, 0.19 atom of  $U^{235}$  will be converted to  $U^{236}$  for each atom that fissions. Thus, total fuel loss is 3.12 percent. The reactivity worth of a uniform 3.12-percent change in fuel loading was calculated to be 1.47-percent  $\Delta k/k$ .

Temperature defect. - The reactivity loss as the result of increasing the reactor temperature from cold-critical to full-power operation is called the temperature defect. Since coolant flow requires a temperature of at least 460 K, this was taken as the base temperature for the cold-critical condition. The temperature defect is caused by increased dimensions, decreased material densities, and Doppler broadening of neutron

absorption resonances. Comparison of criticality calculations at the cold and hot conditions indicates that the reactivity lost from core and fuel expansion is 0.58-percent  $\Delta k/k$  and from coolant expansion is 0.26-percent  $\Delta k/k$ . Material data for these calculations are itemized in table V. Free expansion of all components was assumed. The Doppler effect was estimated from an empirical expression developed from data in reference 16 for the reference-design core materials:

$$\frac{d\rho}{dT} = 0.000217T^{-1} - 0.000728T^{-0.8}$$

where  $d\rho/dT$  is the Doppler coefficient of reactivity in units of  $(\Delta k/k)/K$ , and  $T$  is the temperature in degrees K. The numerical coefficients in this formula have been arbitrarily reduced by a factor of 4 from the calculated values to account for a harder flux spectrum and to more closely approximate EBR-II data. Integration between the temperature limits of 460 and 1200 K results in a 0.25-percent  $\Delta k/k$  reactivity loss due to Doppler effect. Thus, the total temperature defect is -1.09-percent  $\Delta k/k$ .

TABLE V. - MATERIAL DATA FOR TEMPERATURE  
DEFECT CALCULATIONS

Component	Material	Average temperature at full power		Average thermal expansion coefficient, $K^{-1}$
		K	$^{\circ}R$	
Coolant	Li <sup>7</sup>	1194	2150	(a)
Fuel	UN	1228	2210	$8.1 \times 10^{-6}$ (ref. 22)
Radial reflector	TZM	1200	2160	5.3 (ref. 23)
Axial reflector	TZM	1200	2160	5.3
Pressure vessel	T-111	1194	2150	7.0 (ref. 24)

<sup>a</sup>Expansion was obtained by the density change calculated from density =  $0.562 - 0.0001T$  where density is in  $g/cm^3$  and  $T$  is the temperature in degrees K (ref. 25, p. 4).

**Fuel swelling.** - Irradiation damage and fission product buildup cause the UN fuel to swell. The fuel pin is constructed to restrain radial expansion and to allow axial expansion. The extent of this swelling was calculated as a function of fuel burnup with a modified version of the CYGRO computer program (ref. 17). These data are reported as percent change in fuel length (appendix A, fig. 15). Based on the power distribution of the reference design, the axial growth of individual pins varied from 4.7 percent in the center of the core to 0.2 percent in certain drum pins. To account for this in the corre-

sponding criticality calculation, fuel zones were grouped according to percent expansion. Details of this analysis are included in the appendix. The resulting reactivity loss was 0.95-percent  $\Delta k/k$  for an average pin growth of 1.013 centimeters.

Shutdown margin. - The shutdown criterion is that the reactor must be able to attain  $k = 0.99$  when two control drums are stuck in their most reactive position (full-in or  $180^\circ$  from shutdown). Thus, if the assumption is made that the reactivity worth of a drum is independent of the position of any other drum,

$$\left(\frac{\Delta k}{k}\right)_{\text{shutdown}} = 1.01 + \frac{1}{3} \left[ \left(\frac{\Delta k}{k}\right)_{\text{shutdown}} + \left(\frac{\Delta k}{k}\right)_{\text{excess}} \right]$$

Based on the previously determined excess reactivity requirements of 3.51-percent  $\Delta k/k$  plus an estimated contingency of 0.5-percent  $\Delta k/k$ , the required shutdown margin is 3.52-percent  $\Delta k/k$ . This contingency was included to account for calculational uncertainties, fabrication tolerances, and design conservatism.

Total control swing. - Thus, the excess reactivity of 4.01-percent  $\Delta k/k$  and the shutdown margin of 3.52-percent  $\Delta k/k$  indicate a total swing of 7.53-percent  $\Delta k/k$  is required. The corresponding  $k_{\text{excess}}$  is 1.0418 (or a calculated  $k_{\text{excess}}$  of 1.0720 to include the undefined bias). These data represent minimum values that the control system and the reactor must attain.

## Reactivity Control

Considerations from the standpoint of reactor control are stability and shutdown capability. Reactor stability generally requires negative temperature and power coefficients of reactivity. The reactivity change with increasing temperature was previously shown to be negative. A stability study of the reference design was reported in reference 18, in which limits on reactivity addition were calculated for various operating conditions.

The use of  $\text{Li}^7$  as a coolant, with its low absorption cross section, avoids the positive reactivity effect due to coolant expansion sometimes encountered in fast reactor systems. A positive reactivity effect could occur from pin bowing. However, such bowing can be minimized by mechanical design. Since a fast-spectrum reactor will have a neutron lifetime of the order of  $10^{-8}$  seconds, the necessity exists for a rapid shutdown mechanism. The use of rotatable fueled drums for a control system should achieve this purpose.



## Power Distribution

Because creep of the fuel cladding is one of the principal stress limitations in long-lived, high-temperature reactors, power distributions are of particular importance. Power generation determines clad temperature and is directly related to fuel burnup, which in turn produces fuel swelling. The creep-producing stress is caused by fuel swelling, and the resistance to creep is a function of temperature. Based on the reference fuel-pin design, the allowable burnup required to produce 1-percent creep can be calculated as a function of the fuel concentration in a pin. These data were obtained from CYGRO code calculations, the details of which are presented in the appendix. Based on the fuel loading in the reference design, the burnup data were converted to allowable radial power ratio against fuel volume fraction (fig. 5). The axial peak-to-average

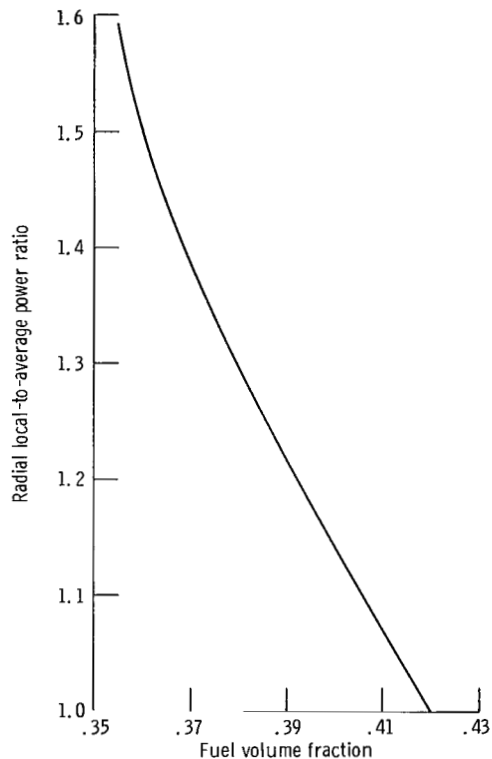


Figure 5. - Allowable radial power ratio to limit fuel cladding creep to 1 percent in 50 000 hours of operation at 2.17 megawatts thermal. Number of fuel pins, 247; average burnup in core, 2.44 percent; average fuel volume fraction in core, 0.385; axial peak-to-average power ratio, 1.23; T-111 clad thickness, 0.147 centimeter (58 mils); tungsten liner thickness, 0.013 centimeter (5 mils).

power ratio was incorporated into the curve in figure 5 because its value is insensitive to radial position and to add some conservatism to the numbers. Fuel zoning will depend on allowable power ratios from figure 5 and the amount of control swing required in the drums.

## DESIGN CALCULATIONS

Design requirements for criticality and control swing were utilized to determine an acceptable fuel loading. Operating characteristics of this core configuration were then determined.

### Reactivity

To meet the required control swing, multiplication constant, and power ratio, a core loading of 0.355 volume fraction of UN in zone I (central 73 pins), 0.377 volume fraction of UN in zone II (adjacent 90 pins), and 0.42 volume fraction of UN in zone III (remaining 18 stationary core pins and 66 drum pins) was calculated. Both the  $k_{\text{excess}}$  of 1.0885 and the control swing of 8.51-percent  $\Delta k/k$  listed in table VI were greater than the required values of 1.0720 and 7.53 percent, respectively. Of the total control swing, 2.64-percent  $\Delta k/k$  was caused by the T-111 poison segment and 5.87-percent  $\Delta k/k$  by the movement of fuel.

TABLE VI. - REACTIVITY OF 0.355, 0.377, 0.42

VOLUME FRACTION URANIUM NITRIDE

CORE LOADING

Calculational model <sup>a</sup>	$k_{\text{shutdown}}$	$k_{\text{excess}}$	Control swing, percent $\Delta k/k$
XY $S_4P_0$ 4 group	-----	1.0907	----
XY $S_2P_0$ 4 group	0.9950	1.0871	8.51
Rθ $S_4P_0$ 4 group	1.0047	1.0985	8.51
XY $S_4P_0$ 13 group	-----	<sup>b</sup> 1.0885	----

<sup>a</sup>All calculations used a reflector savings of 11.738 cm.

<sup>b</sup>Not calculated directly but synthesized from data in table I. This was considered to be the best value for  $k$ .

The calculations made to establish fuel zoning indicated that the UN concentration was limited in the central fuel pins by control swing and in the drum pins by radial power ratio. As the fuel concentration in central pins is increased, the relative amount of fuel in the drums becomes smaller, thereby decreasing drum worth. And for the previously described loading, any increase in fuel concentration of the drum pins would have resulted in a power generation rate that would have exceeded the 1-percent-creep criterion. Considering the steep slope of figure 5, it would appear to be quite difficult to exceed 0.42 UN volume fraction by much and still meet the 1-percent-creep criterion.

Part of this extra control swing will be required for shutdown because of the greater reactivity worth per drum in the reference design. In addition, calculations were performed on the following reactor configurations to check the stuck-drum criterion: (1) two opposite drums rotated in and the other four out, and (2) two adjacent drums rotated in and the other four out. The results, listed in table VII, show that the reactivity worth of

TABLE VII. - REACTIVITY WORTH OF TWO  
CONTROL DRUMS ROTATED FULL IN

Configuration	Worth of two drums, percent $\Delta k/k$
All six drums rotated in	2.84
Two opposite drums rotated in; four drums rotated out	3.16
Two adjacent drums rotated in; four drums rotated out	3.38

a drum is dependent on the position of the other drums. The most severe case, two adjacent drums in, indicates that the shutdown margin must be increased by 0.54-percent  $\Delta k/k$  above the value predicted by one-third of the total drum worth. Thus, the shutdown margin required for the previously described fuel loading is 4.39-percent  $\Delta k/k$ . Incorporation of these data into the total control swing reduces the contingency (uncertainty allowance) to 0.61-percent  $\Delta k/k$  (table VIII). One component of the contingency is the fuel-loading tolerance which, however, has not yet been established quantitatively.

Any extra reactivity in the control swing can either be shimmed out or used to extend lifetime (assuming that other criteria, such as creep, are not exceeded). Life extension would require an additional 0.07-percent  $\Delta k/k$  per 1000 hours based on fuel loss and swelling requirements.

TABLE VIII. - REACTIVITY COMPONENTS  
OF CONTROL SWING

Component	Reactivity, percent $\Delta k/k$
Fuel burnup	1.47
Temperature defect:	1.09
Coolant expansion (0.26)	
Fuel and structure expansion (0.58)	
Doppler (0.25)	
Fuel swelling	.95
Uncertainty allowance	.61
Total excess reactivity	4.12
Shutdown margin	4.39
Total control swing	8.51

Extra  $k$  from the previously described fuel loading can be reduced by replacing fuel pellets with W spacers. Maximum worth of -1.53-percent  $\Delta k/k$  per axial centimeter of fuel occurs at the center of all 247 pins (fig. 6). Fuel replacement at each end of the pins was worth about a factor of 3 less. The axial peak-to-average power ratio was unaffected by end fuel removal and was reduced about 7 percent by central removal of 10 percent of the fuel. This technique can be used to adjust the final core loading prior to assembly.

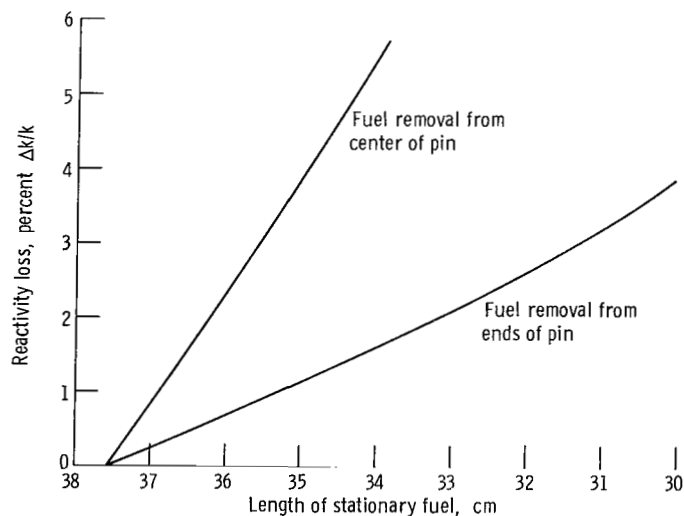


Figure 6. - Reactivity worth of tungsten spacers inserted into all fuel pins.

It is assumed that the reduction of the 1.65-percent  $\Delta k/k$  excess can be achieved without a significant loss in control swing. When fabrication tolerances are included in the analysis for the final core loading,  $k$  will probably be reduced. Additional reduction could result from fuel removal. If necessary, selective fuel removal could be used to enhance control swing; for example, fuel removal from the stationary core would increase the relative amount of fuel in the drums and thus increase control swing.

## Reactivity Control

Control system. - A reactivity control curve was constructed from criticality calculations of a reactor with all control drums rotated to some fixed position between  $0^\circ$  and  $180^\circ$  from shutdown. These results are plotted in figure 7. The close approximation to a  $\sin^2 \theta/2$  function was noted, where  $\theta$  is the degrees of rotation from shutdown. Based on previously described reactivity requirements, drum positions for cold critical and hot critical (beginning of life) were calculated to be  $102^\circ$  and  $118^\circ$  from shutdown, respectively. The highest sensitivity ( $\sim 0.15$ -percent  $\Delta k/k$  per degree) occurs in the  $70^\circ$  to  $110^\circ$  range, with decreasing values as the end points of drum movement are approached.

During reactor operation, reactivity is lost by fuel loss and fuel growth. Reactivity from fuel loss is linear with EFPH (effective full-power hours) at the rate of 0.294-percent  $\Delta k/k$  per 10 000 hours. However, fuel growth is relatively low for the first 20 000 hours and increases to a constant rate after 35 000 hours (appendix A, fig. 16). Incremental data for reactivity use during operation are tabulated in table IX to provide

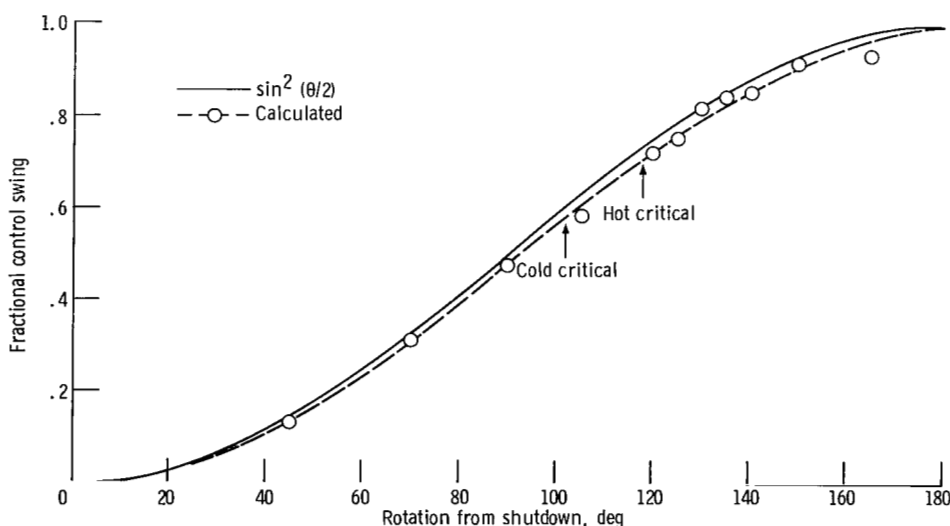


Figure 7. - Control curve for six drums rotated clockwise in unison.

TABLE IX. - REACTIVITY REQUIREMENTS DURING CORE LIFE

	Time interval, <sup>a</sup> hr					
	0 to 10 000	10 000 to 20 000	20 000 to 25 000	25 000 to 30 000	30 000 to 40 000	40 000 to 50 000
Reactivity worth of fuel swelling, percent $\Delta k/k$	0.0285	0.0475	0.057	0.1045	0.3515	0.361
Reactivity worth of fuel burnup, percent $\Delta k/k$	.294	.294	.147	.147	.294	.294
Total reactivity requirement, percent $\Delta k/k$	.3225	.3415	.204	.2515	.6455	.655
Cumulative reactivity requirement from beginning of life, percent $\Delta k/k$	.3225	.664	.868	1.1195	1.765	2.42
Fractional control swing	.0379	.078	.102	.134	.2074	.2843
Drum position, degrees from shutdown	118 to 124	124 to 130	130 to 133	133 to 138	138 to 153	153 to 180

<sup>a</sup>Effective full-power hours (EFPH) of operation.

a basis for determining drum position as a function of core life (fig. 8). Thus, only 24 percent of the drum rotation occurs during the first half of core life.

Kinetics properties. - Two items, prompt neutron lifetime and effective delayed neutron fraction, although generally considered to be kinetics properties can be calculated with static reactor models. Thus, prompt neutron lifetime was calculated with the TDSN neutron transport code using the  $1/v$  absorber technique, which states that the lifetime is directly proportional to the reactivity difference between reactors with and without a pure absorber material. The perturbation method was also used to calculate neutron lifetime, using the PERTRAN code (ref. 19). The calculated value is  $4 \times 10^{-8}$  seconds, which represents a consensus of several calculations using different models (table X).

Using a perturbation technique (ref. 20), a value of 1.014 was calculated for the ratio of effective delayed neutron fraction to absolute delayed neutron fraction  $\beta_{\text{eff}}/\beta$ . Based on an absolute yield of 0.0165 delayed neutrons per fission for fast fission in  $\text{U}^{235}$  (ref. 21, p. 102) and 2.516 total neutrons per fission (calculated for the reference design),  $\beta$  equals 0.0066. The corresponding value for  $\beta_{\text{eff}}$  is 0.0067. For comparative

TABLE X. - CALCULATED VALUES OF  
PROMPT NEUTRON LIFETIME

Calculation model	Prompt neutron lifetime, sec
1D $S_4P_0$ 4-group transport	$43 \times 10^{-9}$
1D $S_4P_0$ 13-group transport	42
RZ $S_4P_0$ 4-group transport	46
1D $P_1$ 4-group perturbation	34

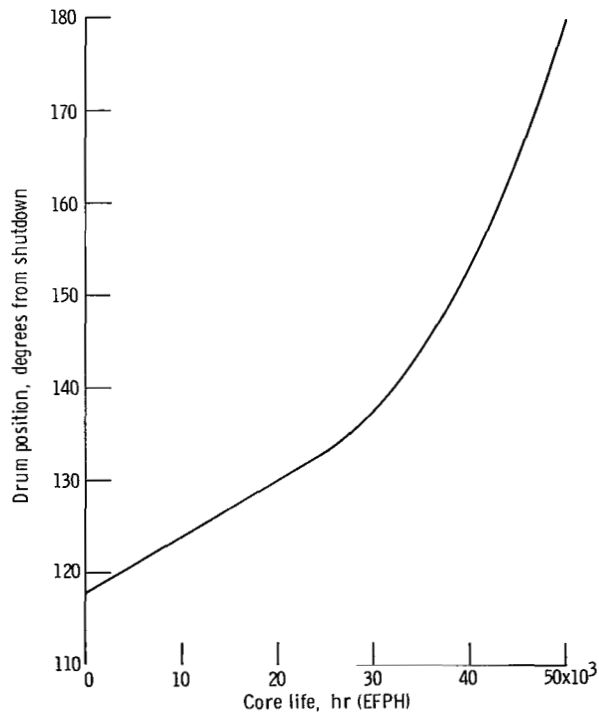


Figure 8. - Drum position during core life.

purposes the experimental lifetime and  $\beta_{\text{eff}}$  values for TOPSY, a natural-uranium-reflected highly enriched sphere, are  $1.8 \times 10^{-8}$  seconds and 0.0072, respectively (ref. 21, p. 180).

Reactor accidents. - A somewhat cursory examination of reactor behavior in special situations was made by calculating the reactivity changes resulting from several accidents. The results, itemized in table XI, indicate no potentially uncontrollable problems. Loss of the  $\text{Li}^7$  coolant caused a 1.52-percent- $\Delta k/k$  loss in reactivity. Water immersion, which could occur during cross-country transportation or as the result of an aborted launch, caused a 0.49-percent- $\Delta k/k$  increase. This increase is within the shutdown capability of the reactor. Fuel melting in the seven central pins would increase reactivity by 0.31-percent  $\Delta k/k$ . The consequence of this is undefined because it is not known what initial conditions will exist to cause the overheating. Fuel-pin bowing under the worst combination of assembly tolerances would increase reactivity by 0.21-percent  $\Delta k/k$ . This, again, is within the limits of the control system.

TABLE XI. - REACTIVITY EFFECT  
OF VARIOUS ACCIDENTS

Accident	Reactivity change, percent $\Delta k/k$	Remarks
Loss of coolant	-1.52	
Water immersion	+0.49	Unshielded configuration used to get maximum effect
Fuel melting	+0.31	Seven central fuel elements melted and fuel slumped to the axial center
Fuel-pin bowing	+0.21	Lateral movement limited to 0.015 cm (6 mils) by mechanical design

## Power Distribution

Axial. - The axial power distribution has the typical chopped cosine shape (fig. 9) and can be represented very closely by the function  $\cos \pi z/1.44L$ , where  $z$  is the axial variable between  $-L/2$  and  $+L/2$  and  $L$  is the reactor height. The peak-to-average power ratio is 1.23. Although this shape was calculated along the axial centerline, little



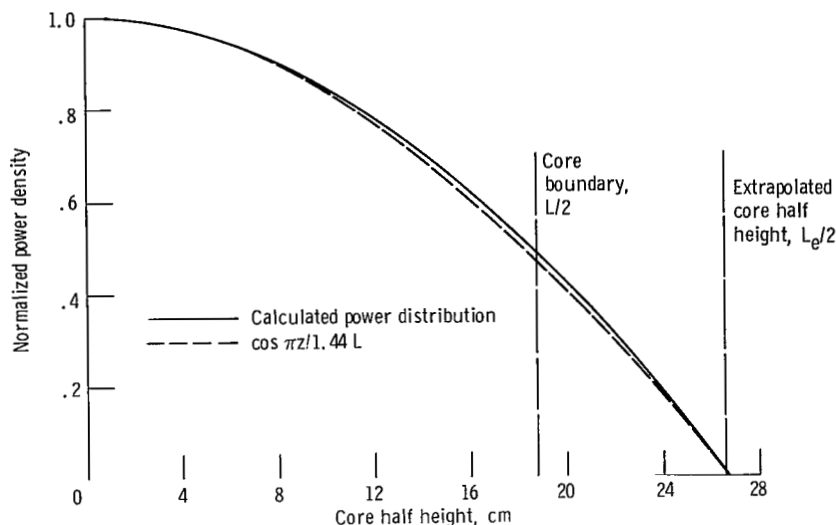
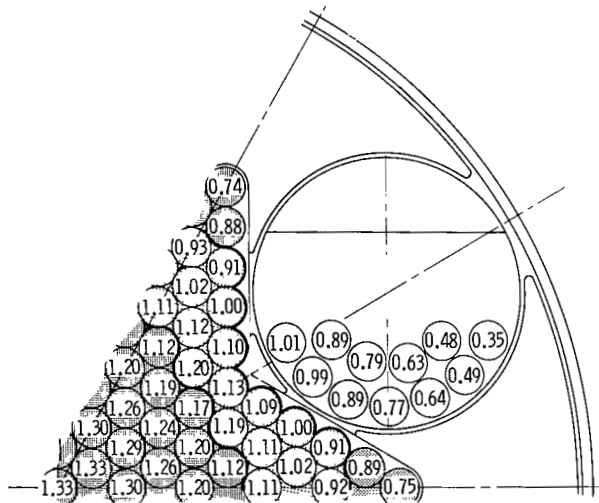


Figure 9. - Axial power distribution at core center.

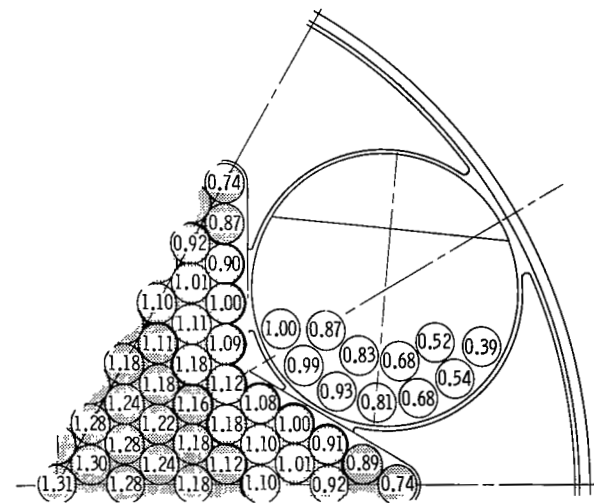
variance was noted at other radial positions. For example, the peak-to-minimum power ratio varied from 2.00 along the centerline to 1.95 in the drum fuel. Thus, it seems reasonable to assume a constant axial shape throughout the following analysis of different radial configurations. Implicit in the power distribution analysis is the assumption that separability into axial and radial functions is valid.

**Radial.** - Because of fuel movement caused by drum rotation, the radial power distribution changes significantly during core life. Radial power maps representing the power generation in each pin (presented as local-to-average power ratio) are included in figure 10 for eight drum positions between beginning and end of life. Changes in radial power between the stationary pins and the drum pins during core life were quite different. Power in the stationary pins was influenced by flux shape and fuel loading, neither of which changed much. For the drum pins, however, an additional factor was the position change which significantly affected the flux environment, thereby changing power generation. Thus, maximum power occurs in the center pin and gradually decreases from 1.33 at the beginning of life to 1.24 at the end of life. Other pins in the stationary section of the core generally show smaller power variations but still show the constantly decreasing trend during core life. Drum pins, however, show greater power changes and have powers that vary inversely with the separation distance between the pin and the center of the core.

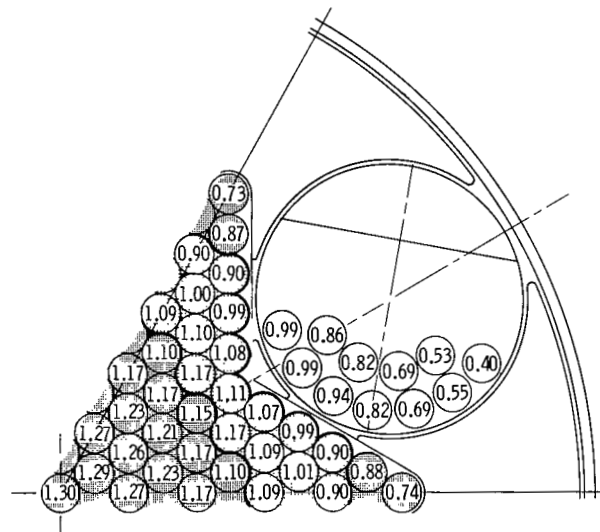
**Creep analysis.** - For use in determining long-time creep behavior, time-averaged power ratios are more appropriate. These values (fig. 11) were obtained by comparing the power distributions in figure 10 to drum position as a function of time. The peak power in each fuel zone is compared in figure 12 to the 1-percent-creep criterion. Cal-



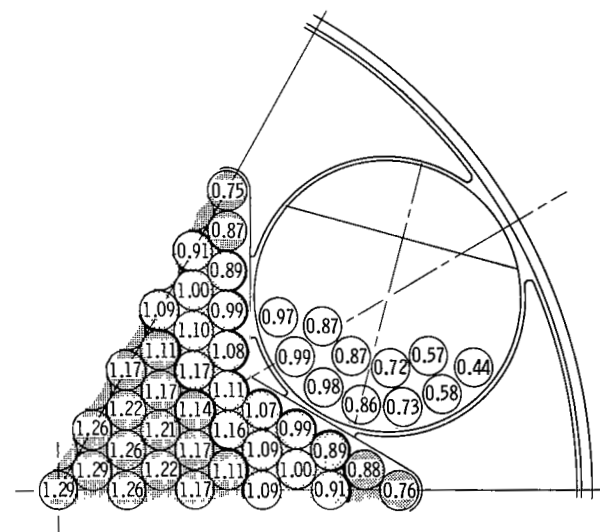
(a) Beginning-of-life drum position (118° from shutdown).



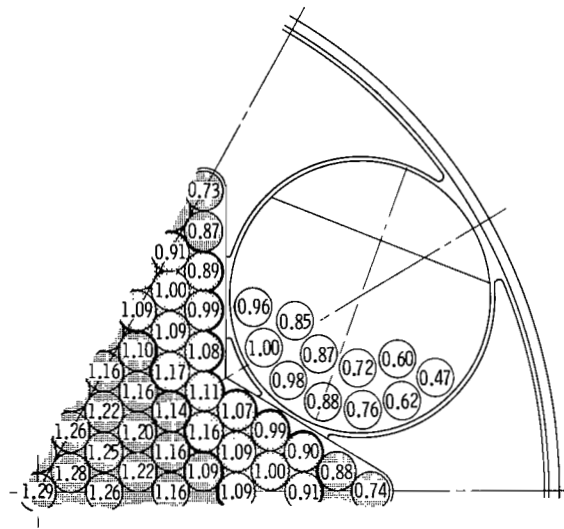
(b) All drums rotated 125° from shutdown.



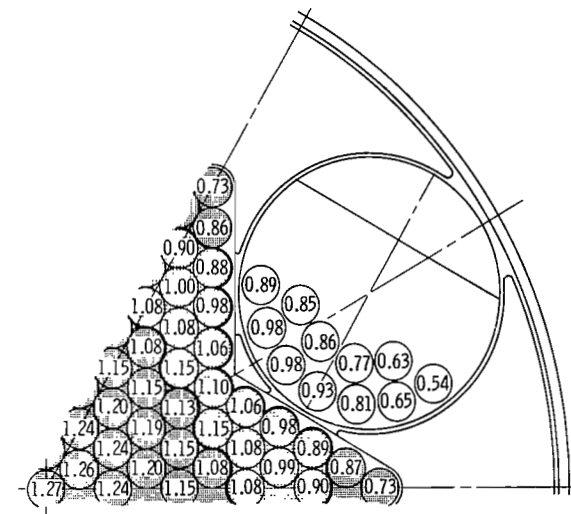
(c) All drums rotated 130° from shutdown.



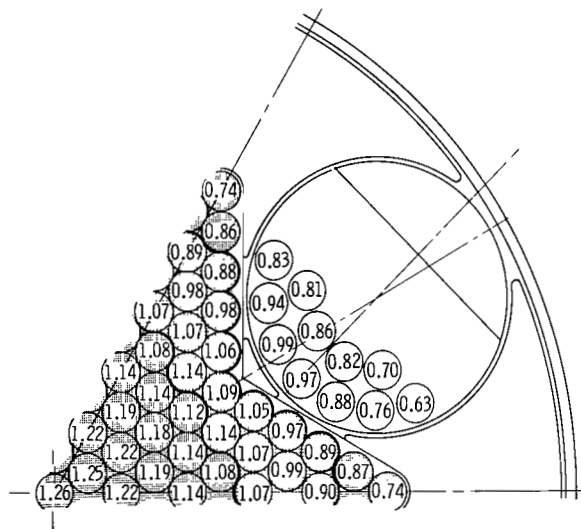
(d) Middle-of-life drum position (135° from shutdown).



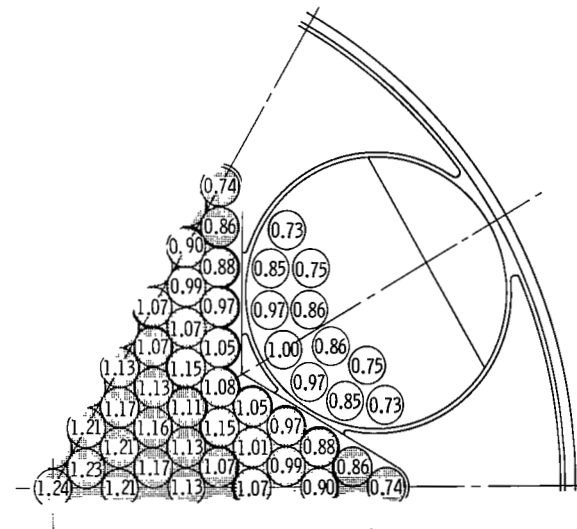
(e) All drums rotated  $140^\circ$  from shutdown.



(f) All drums rotated  $150^\circ$  from shutdown.



(g) All drums rotated  $165^\circ$  from shutdown.



(h) End-of-life drum position ( $180^\circ$  from shutdown).

Figure 10. - Radial power distribution (local-to-average power ratio).

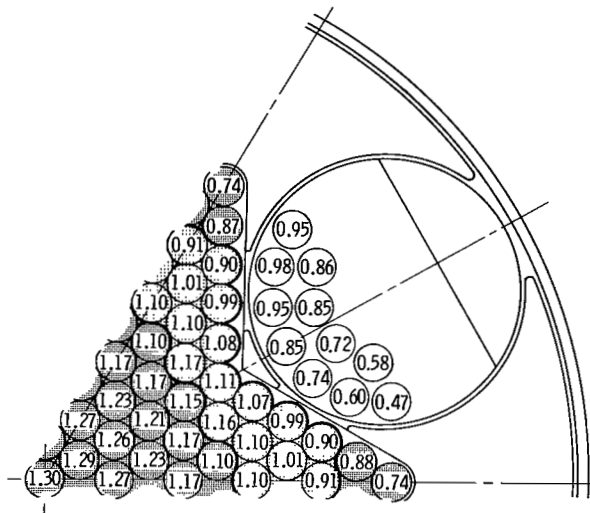


Figure 11. - Radial power ratios averaged over 50 000 effective full-power hours of reactor operation.

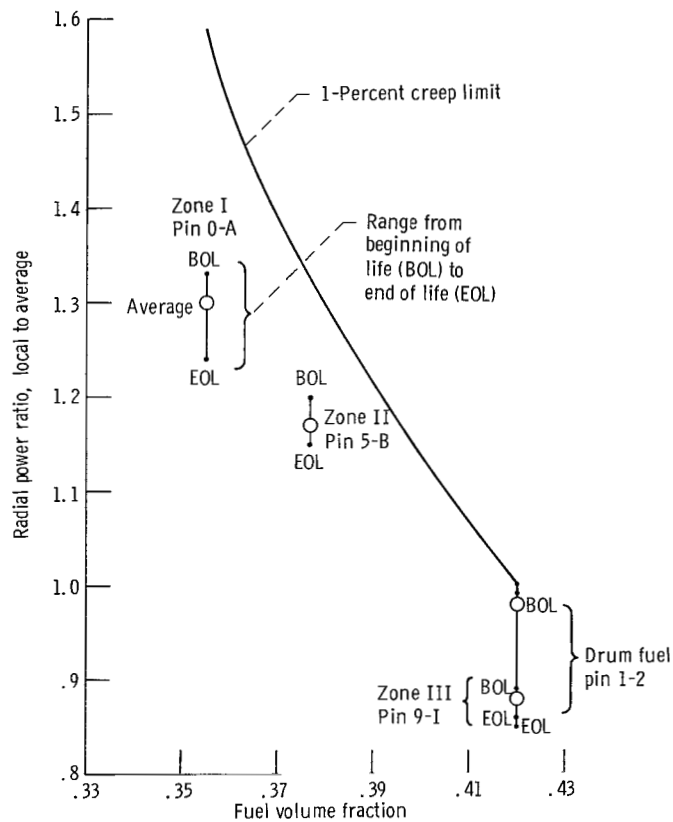


Figure 12. - Calculated radial powers of the peak pin in each fuel zone compared to the creep limited power. Average burnup, 2.44 percent total uranium; average fuel fraction, 0.385; axial peak-to-average power, 1.23.

culated power ratios were 1.30, 1.16, and 0.88 in stationary core zones I, II, and III, respectively, and 0.98 in the control drums. Each is shown to be less than the allowable radial power ratio with the nearest approach being drum pin 1-2 (see appendix B, fig. 18 for pin numbering scheme) at 2 percent less than allowable. Drum pin 1-2 then is the critical pin in this zoning arrangement because any attempt to increase fuel in the stationary pins would decrease the control swing. Additional fuel cannot be added to the drum to compensate without exceeding the creep criterion.

Four-zoned core. - To provide more conservatism in the creep design, a four-zone fuel arrangement might be considered. Because of the relatively high power produced in drum pins 1-1 to 1-4, the fuel loading in those pins was reduced to 0.41 volume fraction of UN. The effect on power distribution and reactivity was calculated using a reactor model with drums in the end-of-life position. Time-averaged radial power ratios were obtained by extrapolation, assuming the same trends as in the reference design. Radial power data for the peak pins in the stationary core and all drum pins are listed in table XII. These data, when compared to the 1-percent-creep curve, indicate the power in the critical drum pin is now 10 percent less than the allowable (fig. 13). Also shown is a more even degree of conservatism between the zones. The reactivity loss in going

TABLE XII. - RADIAL POWER RATIOS IN SELECTED  
PINS OF A FOUR-ZONED REACTOR

Pin location	Pin	Local-to-average power ratio	
		At end of life	Average over life <sup>a</sup>
Center	0-A	1.26	1.32
Zone II	5-B	1.14	1.16
Zone III	9-I	.87	.89
Drum (0.41 UN)	1-1	0.71	0.93
	1-2	.84	.97
	1-3	.95	.93
	1-4	.98	.83
Drum (0.42 UN)	1-5	0.97	0.74
	1-6	.86	.61
	1-7	.73	.47
	2-1	.74	.85
	2-2	.85	.84
	2-3	.86	.72
	2-4	.76	.59

<sup>a</sup>Estimated by assuming the same differential between end of life and average that existed in the reference design.

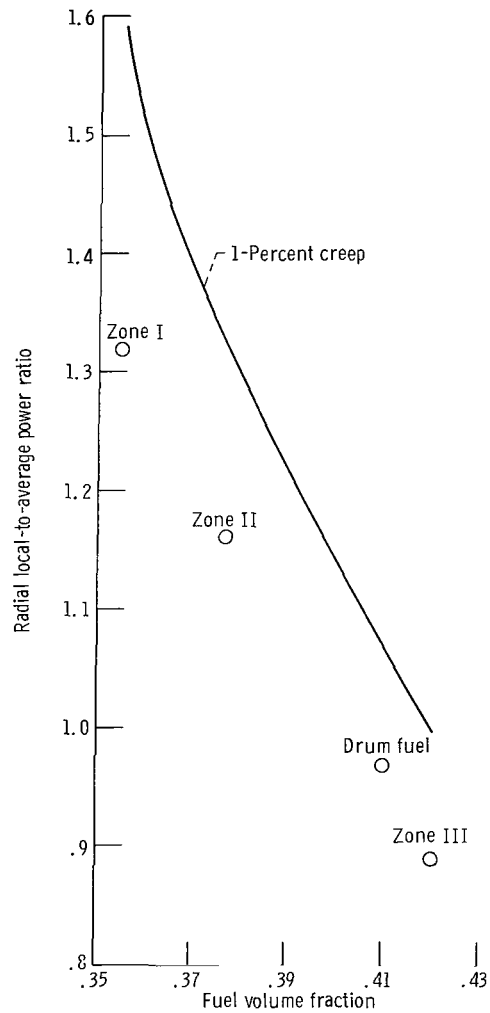


Figure 13. - Peak power ratios in four-zoned core. Number of fuel pins, 247; average burnup in core, 2.44 percent; average fuel volume fraction in core, 0.384; axial peak-to-average power ratio, 1.23; T-111 clad thickness, 0.147 centimeter (58 mils); tungsten liner thickness, 0.013 centimeter (5 mils).

to the four-zone arrangement is 0.10-percent  $\Delta k/k$  in  $k_{\text{excess}}$ , and a somewhat smaller loss in control swing. Thus, a significant improvement in power distribution can be had for a nominal cost in reactivity.

Although the four-zoned fuel distribution is not incorporated into the present reference design, the data are presented herein for subsequent consideration.

## Reactor Characteristics

Ancillary data generated in the various design studies are presented in this section.

Core spectrum. - The average flux spectrum histogram for the fueled portion of the reactor is shown in figure 14. Data were obtained from a 13-group calculation of an end-of-life reactor model. The magnitude of the average flux is  $1.02 \times 10^{14}$  neutrons/(cm<sup>2</sup>)(sec) with a peak-to-average ratio of 1.65, which occurs at the core center. The median flux energy of this spectrum is 0.44 MeV and the median fission energy is 0.36 MeV. These data clearly show the expected fast spectrum for the reference design.

Design coefficients. - A number of reactivity effects have been tabulated which are useful in estimating the import of certain design changes. The data have been fitted to

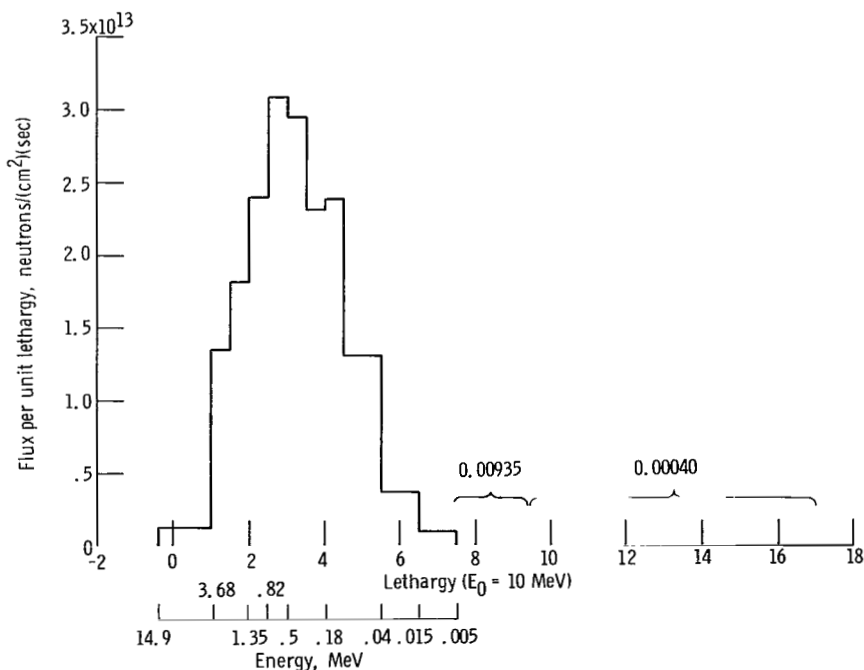


Figure 14. - Average flux spectrum. Average flux,  $\bar{\varphi} = \sum_{u=-0.4}^{\infty} \varphi(u) \Delta u = 1.02 \times 10^{14}$  neutrons/(cm<sup>2</sup>)(sec); 2.17-megawatt-thermal fast reactor; fuel loading: 0.355, 0.377, 0.42 core volume fraction of uranium nitride; number of fuel pins, 247; average energy,  $\bar{E} = 0.44$  MeV.

TABLE XIII. - DESIGN COEFFICIENTS

Property	Coefficient	Formula
Coolant density	0.018	$\frac{\Delta k}{k} = 0.018 \frac{\Delta \rho}{\rho}$
Fuel mass	.47	$\frac{\Delta k}{k} = 0.47 \frac{\Delta M}{M}$
Fuel length	.17	$\frac{\Delta k}{k} = 0.17 \frac{\Delta L}{L}$
Core diameter	.31	$\frac{\Delta k}{k} = 0.31 \frac{\Delta D}{D}$
Operating lifetime	.0328	$\frac{\Delta k}{k} = 0.0328 \frac{\Delta t}{t}$
Isothermal temperature	.0176	$\frac{\Delta k}{k} = 0.0176 \frac{\Delta T}{T}$

the form  $\Delta k/k = C \times (\Delta F/F)$  where  $C$  is the design coefficient and  $\Delta F/F$  is the relative change in some property (see table XIII for properties). Obviously, these formulas have oversimplified the relations between design parameters and reactivity, and therefore their use should be restricted to small changes from the reference design.

## SUMMARY OF RESULTS

Neutronic design calculations on a small, liquid-metal-cooled, fueled-drum-controlled reactor required to operate for 50 000 hours at 2.17 megawatts thermal with a coolant outlet temperature of 1222 K (2200 R) yielded the following results:

1. A radial fuel zoning arrangement of 0.355 volume fraction of uranium nitride (UN) in the central 73 pins, 0.377 volume fraction UN in the intermediate stationary core zone of 90 pins, 0.42 volume fraction UN in the remaining 18 peripheral stationary core pins, and 0.42 volume fraction UN in the 66 drum pins was used. The arrangement provided a control swing of 8.51-percent  $\Delta k/k$  and a multiplication constant of 1.0885, both of which are adequate to operate the reactor.

2. Fuel loading was limited in the drum pins by the 1-percent-creep limit established for the fuel cladding and in the stationary core by the required control swing.



3. The control swing was composed of 1.47-percent  $\Delta k/k$  for fuel burnup, 1.09-percent  $\Delta k/k$  for temperature defect, 0.95-percent  $\Delta k/k$  for axial fuel swelling, 0.61-percent  $\Delta k/k$  for contingency, and 4.39-percent  $\Delta k/k$  for shutdown margin.

4. The shutdown margin includes an allowance to ensure 1-percent  $\Delta k$  subcriticality when two drums are stuck in their most reactive position. Adjacent stuck drums were shown to be worth 0.54-percent  $\Delta k/k$  more than would be predicted on the basis of unit drum worth.

5. The reactivity response curve (control curve) for simultaneous movement of all six control drums indicates that cold- and hot-critical drum positions are  $102^\circ$  and  $118^\circ$  from shutdown, respectively.

6. Peak-to-average radial power ratios (averaged over core life) were 1.30, 1.16, and 0.88 in stationary core zones I, II, and III, respectively, and 0.98 in the control drums.

7. Peak-to-average axial power ratio was 1.23 and its shape could be predicted by the function  $\cos \pi z/1.44L$ .

8. Accident analyses indicated the following reactivity effects: -1.52-percent  $\Delta k/k$  from loss of coolant, 0.49-percent  $\Delta k/k$  from water immersion, 0.31-percent  $\Delta k/k$  from melting of seven central fuel pins, and 0.21-percent  $\Delta k/k$  from fuel-pin bowing.

9. A prompt neutron lifetime of  $4 \times 10^{-8}$  second and an effective delayed neutron fraction of 0.0067 were calculated.

10. Average core flux was  $1.02 \times 10^{14}$  neutrons/(cm<sup>2</sup>)(sec) with a median energy of 0.44 MeV. Median fission energy was 0.36 MeV.

Lewis Research Center,  
National Aeronautics and Space Administration,  
Cleveland, Ohio, September 10, 1970,  
120-27.

## APPENDIX B

### FUEL CLADDING CREEP ANALYSIS

The CYGRO program was also used to calculate radial fuel swelling for the creep analysis. Clad deflection (or creep) was calculated as a function of burnup with fuel loading as a parameter. The 1-percent-creep data were then crossplotted to obtain fuel burnup against fuel volume fraction (fig. 17). A more useful form is to express burnup as radial power ratio, which can be done by

$$\frac{P}{P_R} = \frac{B \times VF_f}{\left(\frac{P}{P}\right)_Z \times \bar{B} \times \overline{VF_f}}$$

where

- B            burnup of a specific pin, percent
- $VF_f$         fuel volume fraction in a specific pin
- $\left(\frac{P}{\bar{P}}\right)_Z$     axial peak-to-average power ratio
- $\bar{B}$            average burnup in core, percent
- $\overline{VF_f}$        average fuel volume fraction in core

The data in figure 17 were determined specifically for 0.44-percent creep. However, lack of knowledge of the creep behavior of T-111 in the range of interest has prompted the use of the calculated stresses as 1-percent-creep limits. This procedure should provide some additional conservatism in the reactor design.

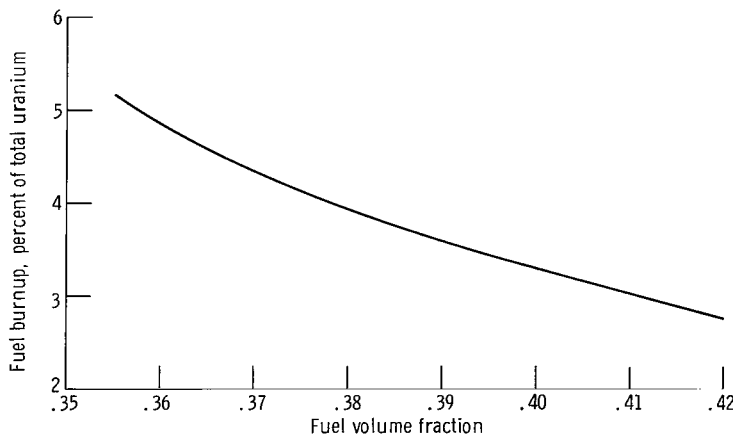


Figure 17. - Fuel burnup required to produce 1-percent creep in fuel cladding.

## APPENDIX C

### RADIAL POWER MAP

To define pin locations, the numbering scheme in figure 18 was used. Only a  $60^\circ$  sector was required because of geometric symmetry.

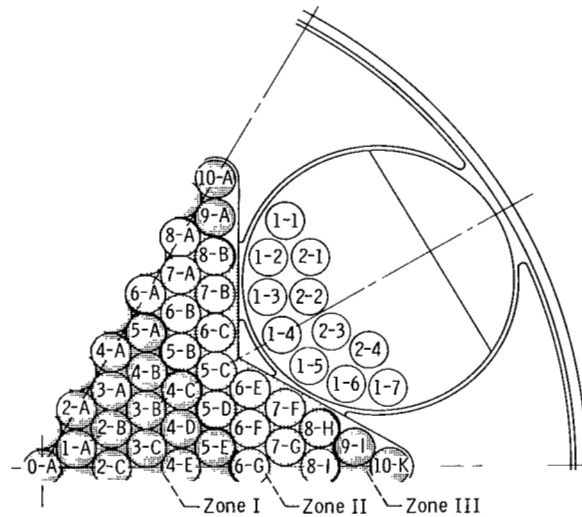


Figure 18. - Numbering scheme for fuel-pin locations.

## APPENDIX D

### MATERIAL WORTHS

In the course of the various design studies a number of miscellaneous material reactivity worths were calculated. These data are itemized in table XV.

TABLE XV. - MATERIAL REACTIVITY WORTHS

Material	Change in reactivity, <sup>a</sup> percent $\Delta k/k$
7.64-cm $\text{Li}^6\text{H}$ radial shield	-0.26
Replacement of void with T-111 fuel cladding, per kg	-.017
Replacement of Mo with $\text{Li}^7$ in reflector region, per percent material	-.06
Replacement of T-111 with Mo in the control drums	+.31
Replacement of T-111 with W-25Re in fuel cladding	+1.57
Axial reflector reduction, cm:	
10.16 to 7.62	-.35
7.62 to 5.08	-.54

<sup>a</sup>Reactor configuration with all drums rotated in.

## REFERENCES

1. Lantz, Edward; Mayo, Wendell; Westfall, Robert M.; and Anderson, John L., Jr.: Small High-Temperature Nuclear Reactors for Space Power. NASA TN D-4371, 1968.
2. Lahti, Gerald P.; Lantz, Edward; and Miller, John V.: Preliminary Considerations for Fast-Spectrum, Liquid-Metal Cooled Nuclear Reactor Program for Space-Power Applications. NASA TN D-4315, 1968.
3. Whitmarsh, Charles L., Jr.; and Kerwin, Paul T.: A 1-Megawatt Reactor Design for Brayton-Cycle Space Power Application. II - Neutronics Design. NASA TN D-5014, 1969.
4. Anderson, John L.; Mayo, Wendell; and Lantz, Edward: Reactivity Control of Fast-Spectrum Reactors by Reversible Hydriding of Yttrium Zones. NASA TN D-4615, 1968.
5. Westfall, Robert M.; and Mayo, Wendell: Neutronic Calculations of Fuel and Poison Drum Control of Refractory-Metal, Fast-Spectrum, Space Power Reactors. NASA TN D-4709, 1968.
6. Mayo, Wendell: Neutronic Effects of Moderator Insertion in Fast-Spectrum Reactors. NASA TM X-1614, 1968.
7. Mayo, Wendell; and Westfall, Robert M.: Radial Power Tailoring for a Uranium Dioxide - T-111 Clad Reactor with Contained Fission Product Gases. NASA TM X-1795, 1969.
8. Whitmarsh, Charles L., Jr.; and Mayo, Wendell: Neutronic Comparison of Beryllium Oxide and Molybdenum for Movable Reflector Control of a Fast-Spectrum Reactor. NASA TM X-1822, 1969.
9. Mayo, Wendell; and Westfall, Robert M.: Reflector-Based Poison-Drum Control on Equal-Size Reactor Cores Fueled with Uranium-233 and with Uranium-235. NASA TM X-1883, 1969.
10. Mayo, Wendell; Whitmarsh, Charles L., Jr.; Miller, John V.; and Allen, Hubert W.: Characteristics of a 2.17-Megawatt Fast-Spectrum Reactor Concept Using an Axially Moving Reflector Control System. NASA TM X-1911, 1969.
11. Barber, Clayton E.: A FORTRAN IV Two-Dimensional Discrete Angular Segmentation Transport Program. NASA TN D-3573, 1966.

12. Soltez, R. G.; Disney, R. K.; and Collier, G.: Users Manual for the DOT-IIW Discrete Ordinates Transport Computer Program. Rep. WANL-TME-1982, Westinghouse Electric Corp., Dec. 1969.
13. Joanou, G. D.; and Dudek, J. S.: GAM-II. A  $B_3$  Code for the Calculation of Fast-Neutron Spectra and Associated Multigroup Constants. Rep. GA-4265, General Atomics Div., General Dynamics Corp., Sept. 16, 1963.
14. Joanou, G. D.; Smith, C. V.; and Vieweg, H. A.: GATHER-II, An IBM-7090 FORTRAN-II Program for the Computation of Thermal-Neutron Spectra and Associated Multigroup Cross-Sections. Rep. GA-4132, General Dynamics Corp., July 8, 1963.
15. Mayo, Wendell; and Lantz, Edward: Analysis of Fuel Loading Requirements and Neutron Energy Spectrum of a Fast Spectrum, Molybdenum-Reflected, Critical Assembly. NASA TM X-52762, 1970.
16. Brehm, Richard L.: Estimates of Doppler Coefficients for In-Pile Thermionic Reactor Materials. Rep. JPL-TR-32-1077, Jet Propulsion Lab., California Inst. Tech. (NASA CR-85358), Oct. 1, 1967.
17. Friedrich, C. M.; and Guilinger, W. H.: CYGRO-2, A FORTRAN-IV Computer Program for Stress Analysis of the Growth of Cylindrical Fuel Elements with Fission Gas Bubbles. Rep. WAPD-TM-547, Westinghouse Electric Corp., Nov. 1966.
18. Niederauer, George F.: Neutron Kinetics of a Fast, Hot, Critical Assembly in the Startup Mode. NASA TM X-2078, 1970.
19. Anderson, John A.: PERTRAN - A Transport-Perturbation Program. NASA TN D-5906, 1970.
20. Perez-Belles, R.; Kington, J. D.; and DeSaussure, G.: A Measurement of the Effective Delayed Neutron Fraction for the Bulk Shielding Reactor-1. Nucl. Sci. Eng., vol. 12, Apr. 1969, pp. 505-512.
21. Keepin, G. Robert: Physics of Nuclear Kinetics. Addison-Wesley Publ. Co., Inc., 1965, p. 102.
22. DeCrescente, M. A.; Freed, M. F.; and Caplow, F. B.: Uranium Nitride Fuel Development - SNAP-50. Rep. PWAC-488, Pratt & Whitney Aircraft, Oct. 1965.
23. Tietz, T. E.; and Wilson, J. W.: Behavior and Properties of Refractory Metals. Stanford Univ. Press, 1965, p. 202.

24. Schmidt, F. F.; and Ogden, H. R.: Engineering Properties of Tantalum and Tantalum Alloys. DMIC-189, Battelle Memorial Inst., Sept. 13, 1963, p. A-88.
25. Davison, Harry W.: Compilation of Thermophysical Properties of Liquid Lithium. NASA TN D-4650, 1968.



03U 001 47 51 3DS 71043 00903  
AIR FORCE WEAPONS LABORATORY /WLCL/  
KIRTLAND AFB, NEW MEXICO 87117

ATT E. LOU BCWMAN, CHIEF, TECH. LIBRARY

POSTMASTER: If Undeliverable (Section  
Postal Manual) Do Not

*"The aeronautical and space activities of the United States shall be conducted so as to contribute . . . to the expansion of human knowledge of phenomena in the atmosphere and space. The Administration shall provide for the widest practicable and appropriate dissemination of information concerning its activities and the results thereof."*

—NATIONAL AERONAUTICS AND SPACE ACT OF 1958

## NASA SCIENTIFIC AND TECHNICAL PUBLICATIONS

**TECHNICAL REPORTS:** Scientific and technical information considered important, complete, and a lasting contribution to existing knowledge.

**TECHNICAL NOTES:** Information less broad in scope but nevertheless of importance as a contribution to existing knowledge.

**TECHNICAL MEMORANDUMS:** Information receiving limited distribution because of preliminary data, security classification, or other reasons.

**CONTRACTOR REPORTS:** Scientific and technical information generated under a NASA contract or grant and considered an important contribution to existing knowledge.

**TECHNICAL TRANSLATIONS:** Information published in a foreign language considered to merit NASA distribution in English.

**SPECIAL PUBLICATIONS:** Information derived from or of value to NASA activities. Publications include conference proceedings, monographs, data compilations, handbooks, sourcebooks, and special bibliographies.

**TECHNOLOGY UTILIZATION PUBLICATIONS:** Information on technology used by NASA that may be of particular interest in commercial and other non-aerospace applications. Publications include Tech Briefs, Technology Utilization Reports and Technology Surveys.

*Details on the availability of these publications may be obtained from:*

**SCIENTIFIC AND TECHNICAL INFORMATION OFFICE**

**NATIONAL AERONAUTICS AND SPACE ADMINISTRATION**

**Washington, D.C. 20546**